Journal of Quantitative Spectroscopy & Radiative Transfer 189 (2017) 344–350

Contents lists available at ScienceDirect

Journal of Quantitative Spectroscopy & Radiative Transfer

journal homepage: www.elsevier.com/locate/jqsrt

High resolution study of the rotational structure of doubly excited vibrational states of $^{32}S^{16}O^{18}O$: The first analysis of the $2\nu_1$, $\nu_1+\nu_3$, and $2\nu_3$ bands

O.N. Ulenikov [a,*], E.S. Bekhtereva [a], O.V. Gromova [a], V.A. Zamotaeva [a], S.I. Kuznetsov [a], C. Sydow [b], S. Bauerecker [b]

[a] Institute of Physics and Technology, National Research Tomsk Polytechnic University, Tomsk 634050, Russia
[b] Institut für Physikalische und Theoretische Chemie, Technische Universität Braunschweig, D-38106, Braunschweig, Germany

ARTICLE INFO

Article history:
Received 17 November 2016
Accepted 15 December 2016
Available online 23 December 2016

ABSTRACT

The high resolution infrared spectra of the $^{32}S^{16}O^{18}O$ molecule were recorded with a Bruker IFS 120 HR Fourier transform interferometer for the first time in the region of 1800–2800 cm^{-1} where the bands $2\nu_1$, $\nu_1+\nu_3$, and $2\nu_3$ are located. About 3970, 2960 and 3450 transitions were assigned in the experimental spectra with the maximum values of quantum numbers $J^{max.}/K_a^{max.}$ equal to 59/20, 68/25, and 43/18 to the bands $2\nu_1$, $\nu_1+\nu_3$, and $2\nu_3$, respectively. The subsequent weighted fit of experimentally assigned transitions was made with the Hamiltonian model which takes into account the resonance interactions between the studied vibrational states. As the result, a set of 39 fitted parameters was obtained which reproduces the initial 3213 ro-vibrational energy values obtained from the assigned transitions with the $d_{rms} = 2.4 \times 10^{-4}$ cm^{-1}.

1. Introduction

Sulfur dioxide is an important species in many fields of study, such as chemistry, interstellar space, planetary nebulae, study of atmospheres of the Earth and Venus, food technology, and many others (see, *e.g.*, Refs. [1–9]). On that reason, high resolution spectra of sulfur dioxide, $^{32}S^{16}O_2$, and its isotopologues, $^{34}S^{16}O_2$ and $^{32}S^{18}O_2$, have been subject of numerous laboratory investigations for a long time (see, e.g., reviews in the recent papers, Refs. [10,11]; see also Ref. [12]). Despite the fact that it is the third most abundant isotopic impurity, 0.2%, in normal samples after $^{32}S^{16}O_2$ and $^{34}S^{16}O_2$ and, as a consequence, one can expect to observe it in the spectra of the atmospheres of the outer planetary bodies, the $^{32}S^{16}O^{18}O$ isotopologue has rarely been investigated up to now, see Refs. [11,13–16].

The present work continues our recent study of the high resolution spectra of sulfur dioxide and its isotopologues in the infrared region, Refs. [17–26], with the $^{32}S^{16}O^{18}O$ molecule in the spectral region of 2100 - 2700 cm^{-1} where the bands $2\nu_1$, $\nu_1+\nu_3$, and $2\nu_3$ are located. Regarding the other isotopologues of sulphur dioxide, this region was discussed earlier in Refs. [27–41]. For $^{32}S^{16}O^{18}O$, the present study is the first attempt to consider the $2\nu_1$, $\nu_1+\nu_3$, and $2\nu_3$ bands. In Section 2 we describe the conditions of our experiment. Description of the experimental spectra and results of assignment of the transitions are given in Section 3. Section 4 presents the theoretical background of the further analysis of experimental data, including the used Hamiltonian model and numerical estimation of the initial values of the rotational and of the main resonance interaction parameters. The results of the analysis and discussion are given in Section 5.

2. Experimental details

The $^{32}S^{16}O^{18}O$ sample was generated in two steps. In the first step the $^{32}S^{18}O_2$ sample gas was produced by controlled isochoric combustion of sulfur ^{32}S (Roth, purity better than 99.999%) in $^{18}O_2$ (Sigma-Aldrich, 99 atom%). The procedure is described in detail in our preceding paper, Ref. [23]. The $^{32}S^{18}O_2$ sample was treated by use of an optical White cell from stainless steel with a base length of one meter at varied optical paths (4 to 24 m) and sample gas pressures (10 to 430 Pa), see Table 1. At typical leak rates of about 10 Pa/d gaseous water from ambient penetrates into the cell so that a partial exchange of oxygen via the forming sulfurous acid takes place. In this way the portion of $^{32}S^{16}O^{18}O$ and later $^{16}O_2$ increases during a preselected reaction time and the measuring

* Corresponding author.
E-mail address: Ulenikov@mail.ru (O.N. Ulenikov).

http://dx.doi.org/10.1016/j.jqsrt.2016.12.019
0022-4073/

Table 1
Experimental setup for the spectral region 1800–2800 cm^{-1} of the infrared spectrum of $^{32}S^{16}O^{18}O$.

Spectr.	Region/cm^{-1}	Resolution/cm^{-1}	Measuring time/h	No. of scans	Source	Detector	Beam-splitter	Opt. path-length/m	Aperture/mm	Temp./°C	Pressure/Pa	Calibr. gas
I	1800–2800	0.0025	43	1080	Globar	InSb	CaF_2	4	1.00	25 ± 0.5	10	N_2O
II	1800–2800	0.0025	11	280	Globar	InSb	CaF_2	16	1.00	25 ± 0.5	52	N_2O
III	1800–2800	0.0025	23	580	Globar	InSb	CaF_2	24	1.15	25 ± 0.5	280	N_2O
IV	1800–2800	0.0025	21	520	Globar	InSb	CaF_2	24	1.30	25 ± 0.5	430	N_2O

time (11 to 43 h) and a recording period over a few hours could be achieved in which the portion of the here favored $^{32}S^{16}O^{18}O$ isotopologue appeared to be rather constant between 30 and 40% of the total sulfur dioxide.

In the spectral region between 1800 and 2800 cm^{-1} four spectra have been recorded with a Bruker IFS120HR Fourier transform infrared spectrometer in combination with the described White cell. A globar radiation source (driven at 24 V, 3.8 A and about 1 Pa N_2 atmosphere), KBr windows, a CaF_2 beamsplitter and an indium antimonide (InSb) semiconductor detector have been used for recording the spectra. The whole spectrometer was pumped by a turbomolecular pump to an average pressure below 0.1 Pa. The transmission spectrum was obtained by division of the highly resolved single-channel spectrum by a background spectrum with a lower resolution of 0.1 cm^{-1} (averaged by 200 scans). Using Norton-Beer weak apodization, the nominal optical resolution was 0.0025 cm^{-1} for all the spectra, defined by $0.9 \times 1/d_{MOPD}$ (maximum optical path difference) which leads to an instrumental linewidth of 0.002 cm^{-1}. The Doppler broadening for $^{32}S^{16}O^{18}O$ at 298.15 K was between 0.0027 cm^{-1} (at 1800 cm^{-1}) and 0.0042 cm^{-1} (at 2800 cm^{-1}). The pressure broadening was between 0.00003 and 0.0014 cm^{-1} at the used pressure range between 10 and 430 Pa. This means that it has a minor but not neglectable contribution to the total line widths which result between 0.0034 and 0.0049 cm^{-1} (root sum square approximation of convolution) and which is in accordance with the experimental results. The measuring time was about 2.4 min per scan resulting in measuring times between 11 and 43 hours. The spectra were calibrated with N_2O lines at a partial N_2O pressure of about 10 Pa. For optimization of data recording and line calibration we used procedures described in Refs. [42,43].

3. Description of the spectra and assignment of transitions

The survey spectra I and III (for the experimental conditions, see Table 1) in the region of 2100–2700 cm^{-1} are shown in Fig. 1 (reproduced from Ref. [37]). Bands of three isotopic species, $^{32}S^{16}O_2$, $^{32}S^{18}O_2$ and $^{32}S^{16}O^{18}O$, are seen in both spectra. However, as one can see from comparison of spectra I and III, the abundance of $^{32}S^{16}O^{18}O$ in the sample III is higher than in sample I. So the $2\nu_1$ band of $^{32}S^{16}O^{18}O$ (band center near 2240 cm^{-1}) is considerably better pronounced in spectrum III. In spectrum III, one can also recognize the $2\nu_3$ band with the band center near 2675 cm^{-1} which is not visible in spectrum I. The $\nu_1 + \nu_3$ band is clearly pronounced in spectrum I and saturated in spectrum III. As an illustration, the second and third traces in Figs. 2 and 3 show the $\nu_1 + \nu_3$ and $2\nu_3$ bands with highly resolved parts of the experimental spectra in more detail. In the third traces of Figs. 2 and 3 one can see clearly pronounced cluster structures of the Q-band transitions in both bands.

The $^{32}S^{16}O^{18}O$ molecule is an asymmetric top with the value of the asymmetry parameter $\kappa = (2B - A - C)/(A - C) \simeq -0.945$ and with the symmetry isomorphic to the C_s point symmetry group. As the consequence,

1). all three vibrational coordinates, q_1, q_2, and q_3, are symmetric, and all the vibrational states of the $^{32}S^{16}O^{18}O$ molecule are the states of the A' symmetry;

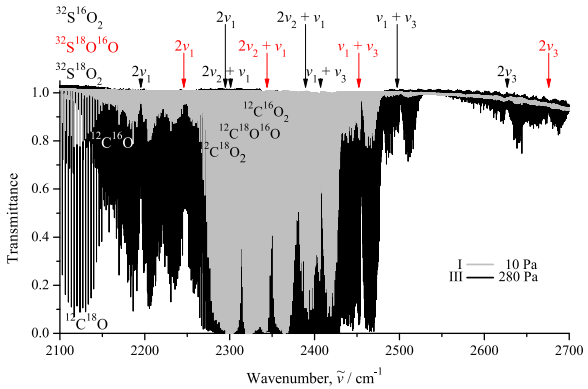

Fig. 1. Survey spectra I and III of $^{32}S^{16}O^{18}O$ in the region of 2100–2700 cm^{-1}. Experimental conditions for the spectrum I: sample pressure is 10 Pa, absorption path length is 4 m; room temperature; number of scans is 1080. Experimental conditions for the spectrum III: sample pressure is 280 Pa, absorption path length is 24 m; room temperature; number of scans is 580.

2). in the *A*-reduction and I^r representation (see, *e.g.*, Refs. [44–47]) three components of the angular momentum operator, J_x, J_y, and J_z, are transformed in accordance with irreducible representations A'', A', and A'', respectively. In accordance with the same irreducible representations, A'', A', and A'', the values k_{zx}, k_{zy}, k_{zz}, are transformed;.

3). as the consequence, any vibrational band of $^{32}S^{16}O^{18}O$ is a hybrid band, Refs. [48–51], and transitions of both the *a*-, and *b*-type are allowed by the symmetry of the molecule; selection rules in this case are: $\Delta J = 0, \pm 1$ and $\Delta K_a = 0, \pm 1, \pm 2, \pm 3, \ldots, \Delta K_c = \pm 1, \pm 3, \ldots$ for any vibrational band of $^{32}S^{16}O^{18}O$.

Assignment of transitions was made on the basis of the Ground State Combination Differences (GSCD) method. In this case, the ground state rotational energies have been calculated with the parameters from Ref. [16] (for the convenience of the reader, parameters of the ground vibrational state from Ref. [16] are reproduced in column 2 of Table 2). As the result, about 3970, 2960 and 3450 transitions with values of quantum numbers $J^{max.}/K_a^{max.}$ equal to 59/20, 68/25, and 43/18 were assigned to the $2\nu_1$, $\nu_1 + \nu_3$, and $2\nu_3$ bands, respectively (see also statistical information in Table 3). The list of assigned transitions is presented in the Supplementary Material.

4. Hamiltonian model and estimation of spectroscopic parameters

4.1. Effective Hamiltonian

The effective Hamiltonian model, which was used for theoretical analysis of experimental data, has been discussed in the preceding studies (see, *e.g.*, Refs. [52–55]). For that reason we reproduce it here without detailed explanations. For the (200), (101) and (002) vibrational states of the $^{32}S^{16}O^{18}O$ molecule it is possible to show that the Coriolis resonance interactions between them are not neglectable and therefore should be taken into account for the

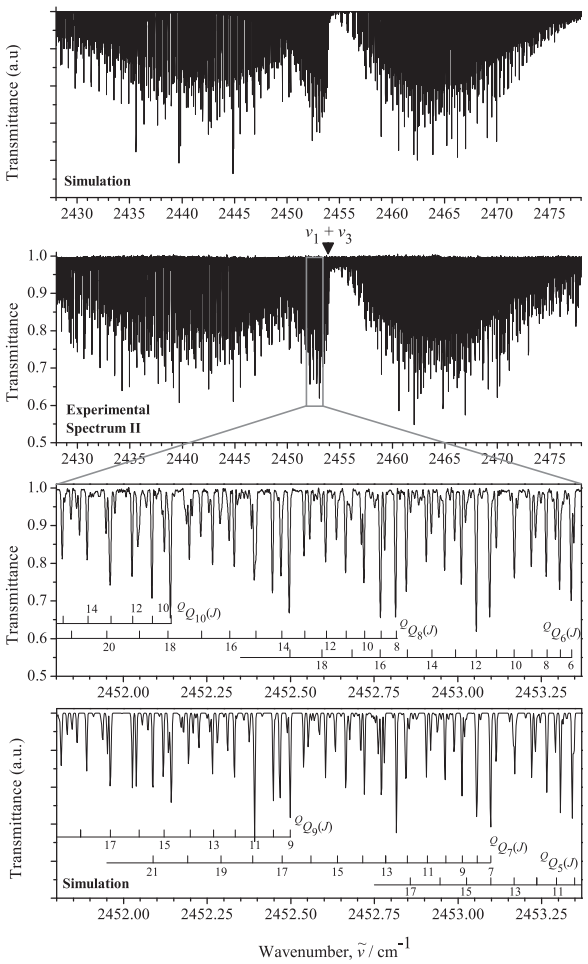

Fig. 2. Low-resolution (second trace) and small part of the high-resolution (third trace) spectrum II in the region of the $\nu_1+\nu_3$ band of $^{32}S^{16}O^{18}O$ (for the experimental conditions, see Table 1). Some sets of transitions of the Q-branch are marked. The first and fourth traces show the simulated spectrum (see text for details of simulation).

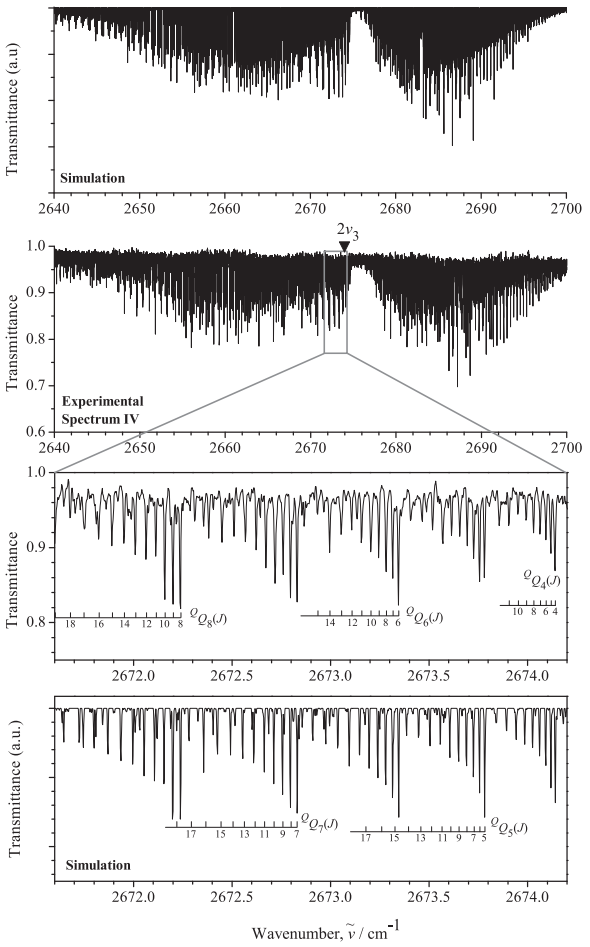

Fig. 3. Low-resolution (second trace) and small part of the high-resolution (third trace) spectrum IV in the region of the $2\nu_3$ band of $^{32}S^{16}O^{18}O$ (for the experimental conditions, see Table 1). Some sets of transitions of the Q-branch are marked. The first and fourth traces show the simulated spectrum (see text for details of simulation).

analysis of the ro-vibrational structures of these vibrational states. On the other hand, interactions between stretching and bending excited states of the molecule are small and can be neglected. As the consequence, the effective Hamiltonian in the form

$$H^{vib.-rot.} = \sum_{v,\tilde{v}} |v\rangle\langle\tilde{v}|H^{v\tilde{v}} \tag{1}$$

can be used in the theoretical analysis of the experimental data. In this case, the summation is taken from 1 to 3 for both v and $\tilde{v}$ in Eq. (1), and $|1\rangle = (200)$, $|2\rangle = (101)$, and $|3\rangle = (002)$. Diagonal blocks H^{vv} ($v = 1, 2, 3$) in Eq. (1) describe the unperturbed rotational structures of the corresponding vibrational states and have the following form of the reduced effective Hamiltonian in the A-reduction and I^r representation (see, *e.g.*, Refs. [56–58]):

$$\begin{aligned} H^{vv} = {} & E^v + \left[A^v - \frac{1}{2}(B^v + C^v)\right]J_z^2 + \frac{1}{2}(B^v + C^v)J^2 + \frac{1}{2}(B^v - C^v)J_{xy}^2 \\ & - \Delta_K^v J_z^4 - \Delta_{JK}^v J_z^2 J^2 - \Delta_J^v J^4 - \delta_K^v\left[J_z^2, J_{xy}^2\right]_+ - 2\delta_J^v J^2 J_{xy}^2 \\ & + H_K^v J_z^6 + H_{KJ}^v J_z^4 J^2 + H_{JK}^v J_z^2 J^4 + H_J^v J^6 \\ & + \left[J_{xy}^2, h_K^v J_z^4 + h_{JK}^v J^2 J_z^2 + h_J^v J^4\right]_+ + L_K^v J_z^8 + L_{KKJ}^v J_z^6 J^2 + L_{JK}^v J_z^4 J^4 \\ & + L_{KJJ}^v J_z^2 J^6 + L_J^v J^8 + \left[J_{xy}^2, l_K^v J_z^6 + l_{KJ}^v J^2 J_z^4 + l_{JK}^v J^4 J_z^2 + l_J^v J^6\right]_+ \\ & + P_K^v J_z^{10} + P_{KKKJ}^v J_z^8 J^2 + P_{KKJJ}^v J_z^6 J^4 + \cdots, \end{aligned} \tag{2}$$

where $J_{xy}^2 = J_x^2 - J_y^2$; $[\ldots, \ldots]_+$ denotes anticommutator; A^v, B^v, and C^v are the effective rotational constants connected with the vibrational state (v), and the other parameters are the different order centrifugal distortion coefficients. The nondiagonal block $H^{v\tilde{v}}$ ($v \neq \tilde{v}$) describes resonance interactions between vibrational states (200) and (101), (101) and (002), and have the form, Ref. [59]

$$H^{v\tilde{v}} = H_F^{v\tilde{v}} + H_{Cy}^{v\tilde{v}}, \tag{3}$$

and the two operators at the right side of Eq. (3) describe Fermi-and Coriolis-type resonance interactions:

$$H_F^{v\tilde{v}} = {}^{v\tilde{v}}F_0 + {}^{v\tilde{v}}F_K J_z^2 + {}^{v\tilde{v}}F_J J^2 + \cdots + {}^{v\tilde{v}}F_{xy}\left(J_x^2 - J_y^2\right) + \cdots \tag{4}$$

and

$$H_{Cy}^{v\tilde{v}} = iJ_x H_{v\tilde{v}}^{(1)} + H_{v\tilde{v}}^{(1)} iJ_x + \left[J_y, J_z\right]_+ H_{v\tilde{v}}^{(2)} + H_{v\tilde{v}}^{(2)}\left[J_y, J_z\right]_+ + \cdots, \tag{5}$$

where

$$H_{v\tilde{v}}^{(i)} = \frac{1}{2}{}^{v\tilde{v}}C^i + {}^{v\tilde{v}}C_K^i J_z^2 + \frac{1}{2}{}^{v\tilde{v}}C_J^i J^2 + {}^{v\tilde{v}}C_{KK}^i J_z^4 + {}^{v\tilde{v}}C_{KJ}^i J_z^2 J^2 + \frac{1}{2}{}^{1\,2}C_{JJ}^i J^4 + \cdots \tag{6}$$

4.2. Estimation of spectroscopic parameters

The energy values obtained from experimental infrared transitions were used then in the weighted fit of parameters of the